Electrodeposition

DOI: 10.1002/anie.201306334

Reliable Metal Deposition into TiO_2 Nanotubes for Leakage-Free Interdigitated Electrode Structures and Use as a Memristive Electrode**

*Ning Liu, Kiyoung Lee, and Patrik Schmuki**

Over the past decades, electrodeposition into ordered nanoporous, nanochanneled, or nanotubular substrates[1–7] has been widely explored and exploited. In this regard, the use of ordered oxide or polymer membranes with pore diameters in the nanometer range as a template for the fabrication of metal or semiconductor nanowires or nanotubes (NTs) is most straightforward. In these cases, deposition is mostly followed by a selective dissolution of the template to obtain a free-standing array of the 1D material of interest. Such attempts were pioneered by the groups of Uosaki,[1] Martin,[2] Masuda,[3] Moskovits,[4] and Gösele,[5,6] who mostly used self-organized porous alumina or track-etched polycarbonate membranes as templates.

While deposition into these electrically insulating materials is comparably well established, it is much less explored for semiconductive substrates,[7] although particularly in the latter case, the properties of the composite, that is, the combination of the deposit and surrounding semiconducting template, are of key interest. For example, in the fabrication of functional core–shell structures, heterojunctions, and interdigitated electrode arrays, the combination of utilized materials provides the functionality. For interdigitated electrode configurations, it is of utmost importance to be able to achieve deposition into the semiconductive template without any through-plating defects, as these would lead to short-circuited spots and thus to failure or drastic performance losses in the devices.

Self-organized nanotubular structures of TiO_2 (a semiconductive substrate), formed by electrochemical anodization, have become some of the most interesting self-organized 1D materials, particularly because these structures offer a unique combination of a wide-band-gap semiconductor with high electron diffusion length and a precisely controllable morphology.[8–13] Moreover, a considerable potential for these nanotube layers lies indeed in a complete filling of the TiO_2 tubes to form interdigitated electrodes for functional solid-state devices. One of the largest potentials of metal-filled tubes may lay in their use as memristive elements.[14] The memristive behavior of thin TiO_2 layers is currently intensively investigated and applied in view of high-density storage devices.[14] These devices rely on a vacancy distribution across the oxide layer that can be switched with a high electric field from a percolating high-conductivity state to a nonpercolating low-conductivity state. To achieve high fields with a moderate voltage, the oxide layer should be sufficiently thin. To exploit a nanotubular geometry for such devices, where each tube is one electrode, and the thin oxide layer at the bottom of the tube is the active switching element, the tube bottom needs to be reliably contacted from the top. Although particle decoration of the tubes can be achieved in a number of quite facile ways (such as impregnation),[15–19] complete filling of the empty tube space on the substrate is not as straightforward as, for example, in the case of alumina,[5] because of the semiconductive nature of TiO_2.[13] Several filling-by-electrodeposition approaches have been reported; in the most recent case, the tube layers were lifted off from the metal substrate, opened at the bottom, and the oxide tubes were filled from an evaporated-noble-metal contact by electrodeposition (in analogy to a treatment often used for porous alumina[3]).[20] Nevertheless, this treatment does, of course, not lead to the desired interdigitated structure. Earlier reports showed filling of amorphous (as formed) TiO_2 nanotubes, but filling of annealed tubes, that is, crystalline tubes in their most functional anatase or rutile form, failed.[13]

Almost any type of photoelectrochemical or solid-state device requires anatase tubes to achieve a reasonable electron-transport performance and a well-defined n-type semiconductive behavior. The latter is the key obstacle for electrodeposition of metals into a layer of intact tubes. The required cathodic potentials switch the n-type material to a "conductive" state (forward-biased semiconductor/electrolyte junction), and as a result deposition does not start at the bottom of the tube, but on the entire surface (see Figure S1a in the Supporting Information). Moreover, thermal annealing of the amorphous layer to anatase always induces some microscopic cracks in the TiO_2 layer. As a result, even if the tube filling is achieved using refined pulse techniques, virtually all the structures show a high degree of short-circuiting (see Figure 1). Characterization after various deposition approaches showed that the typical origin of shorted circuits is the deposition that penetrates the oxide at the bottom of the tube at a weak spot (or crack) and then undermines the tubular layer (Figure 1a,c, and e). Cracking or defects at the bottom may be related to the fluoride-rich layer present at the bottom of the nanotubes,[9] weakening the mechanical or chemical stability of the layers.

[*] Dr. N. Liu, K. Lee, Prof. Dr. P. Schmuki
Department of Materials Science WW4-LKO
University of Erlangen-Nuremberg
Martensstrasse 7, 91058 Erlangen (Germany)
E-mail: schmuki@ww.uni-erlangen.de

[**] We gratefully acknowledge the DFG, especially the Cluster of Excellence (EAM), for financial support.

Supporting information for this article is available on the WWW under http://dx.doi.org/10.1002/anie.201306334.

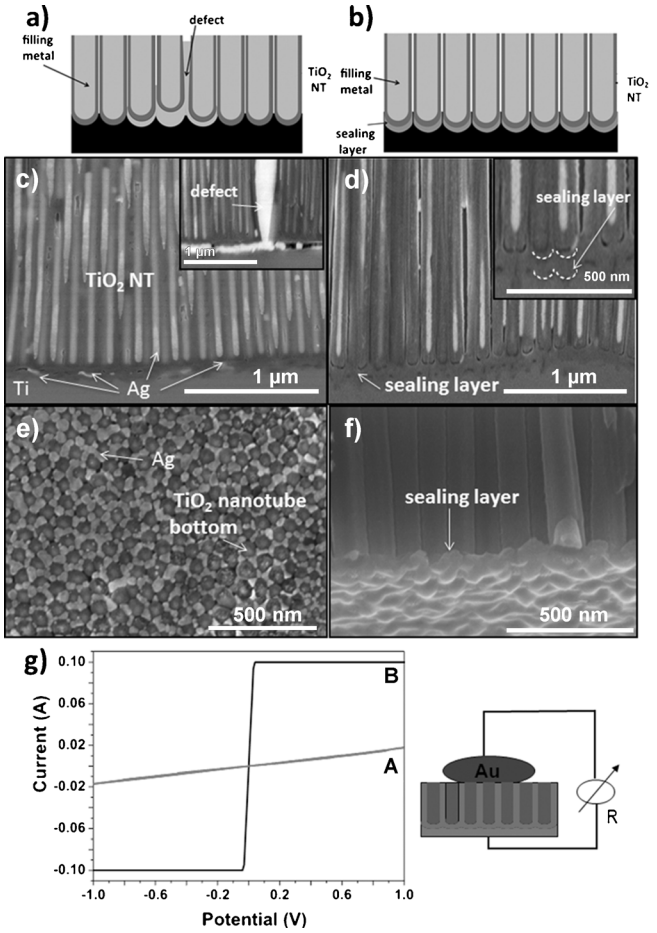

Figure 1. Schematic illustration of electrodeposition into TiO_2 nanotubes a) with conventional defects and b) with a sealing layer underneath the tube layer; SEM cross-sectional images of Ag-filled TiO_2 nanotubes c) without and d) with a sealing layer; e) SEM image of the bottom of Ag-filled TiO_2 nanotubes without sealing, showing leaking of the deposit at interface locations; f) SEM image of the sealing layer underneath the tube layer anodized in ethylene glycol with H_3PO_4; g) I–V curves of Ag-filled TiO_2 nanotubes with (A) and without (B) sealing layers.

Herein, we demonstrate the sealing of defects and deposition of metal into annealed TiO_2 nanotubes, and thus the fabrication of short-circuit-free interdigitated electrode configurations, which can, for example, be used to manufacture a functional memristive electrode. The key steps of our approach are the self-aligned defect-sealing treatment of the bottom of the nanotubes, followed by metal deposition using optimized pulsed electrodeposition. By using this approach, we reached nearly 100% filling of the tubes with any of the explored metals, including Ag, Cu, Au, and Pt, which all result in well-defined electrical properties of the metal/oxide junctions.

We used typical TiO_2 nanotubes, produced in ethylene glycol electrolyte with the addition of NH_4F and deionized H_2O. Figure S2 shows scanning electron microscopy (SEM) top-view and cross-section images of TiO_2 nanotubes with a length of around 3 μm and a tube diameter of approximately 80 nm. After the formation of the tubes, we explored different approaches to seal the defects. An optimized secondary anodization under conditions that lead to a compact oxide layer was clearly most successful. This anodic approach has the advantage that the tube layer will be preferentially oxidized at any defect site, that is, oxide is formed exactly where it is desired, which is at the location of the defect. Nevertheless, in order to completely seal any defects, we had to optimize the sealing process by a secondary anodization (see Table S2 and Figure S3 in the Supporting Information). An optimum sealing was achieved by anodizing in a solution of ethylene glycol and H_3PO_4, as this electrolyte allows the application of sufficiently high voltages to form a coherent and conformal oxide layer underneath the nanotubes, without leading to significant evolution of gaseous oxygen during the process. Water-based electrolytes undermined the nanotube layers and led to their lift-off during sealing or electrodeposition. Figure 1 f shows an optimized sealing layer with a thickness of approximately 50 nm, formed in ethylene glycol/H_3PO_4 electrolyte at 20 V. This layer is uniformly present at the tube bottoms (Figure 1 f) and particularly seals the locations between tubes and cracks.

In order to achieve complete filling of the tubes during electrodeposition, we adopted a strategy that is different from the usual procedures used for the filling of insulating tubes. In the traditional approach, the goal is to initiate the deposition of nuclei at the bottom of the tube and then to continuously fill up the tubes from this point, which is comparably easy if the tube walls are insulating and a conductive bottom can be established. Because of the reasons outlined above, this is not really possible with n-type conductive tubes. Therefore, we changed the strategy and tried to initiate the formation of nuclei over the entire tube wall and then let these nuclei grow together to fill the tubes (concept illustrated in Figure 2). Indeed, the use of an adequate initial pulse leads to homogeneous formation of nuclei all over the tube walls, inside as well as outside (see Figure 2 a). These nuclei can then be grown to coalescence in further current pulses (details about the pulsing procedure given in the Supporting Information). The TiO_2 templates obtained after electrodeposition were examined by SEM to determine the degree of tube filling. Figure 1 c–f shows SEM images of TiO_2 tubes after Ag deposition without (Figure 1 c and e) and with (Figure 1 d and f) a sealing layer present. The cross-sectional SEM images were taken after cross-sectioning the sample by ion milling. As can be seen, both samples show almost 100% Ag filling over the entire TiO_2 nanotube template. In the absence of a sealing layer, Ag penetration through the bottom occurs (Figure 1 c and e), whereas the presence of the sealing layer prevents Ag penetration to the substrate (Figure 1 d).

Dark current–coltage (I–V) characteristics were measured for the Ag-filled TiO_2 nanotubes with and without sealing layers (Figure 1 g). The resistivity of the deposited sample with a sealing layer is approximately 1500 Ωm, while the deposited sample without a sealing layer shows a short-circuit behavior of a connected Ag wire (< 0.1 Ωm). The evaluated resistivity of 1500 Ωm represents essentially the resistivity of the TiO_2 nanotube bottom; considering the dimensions, the result is well within the range of reported values for anatase.[21]

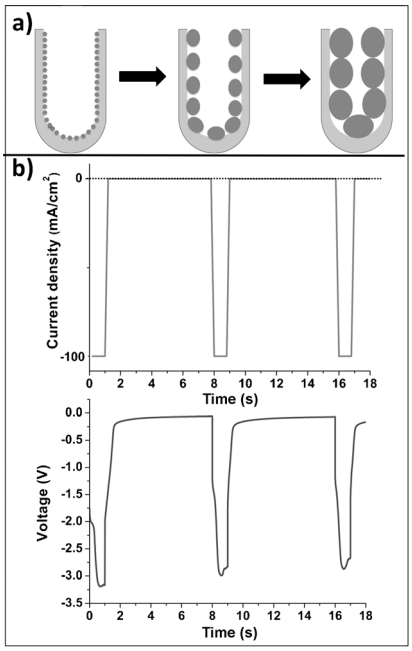

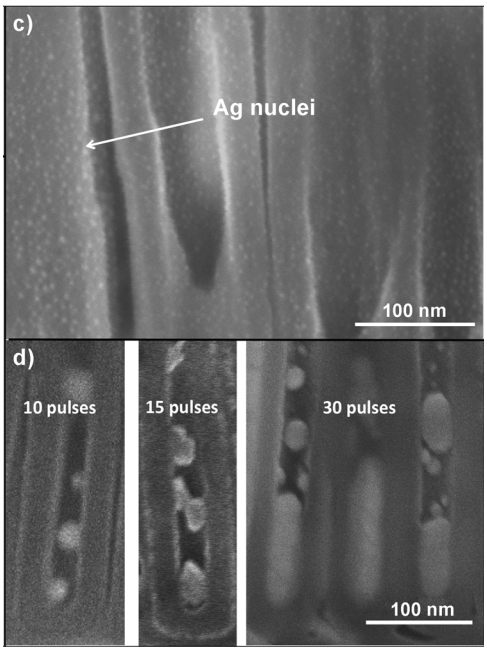

Figure 2. a) Schematic illustration of nuclei formation over the entire tube wall and growth to coalescence; b) voltage pulses and current responses during Ag deposition according to protocol descried in the Supporting Information; c) morphology of the Ag nuclei that are formed after the initial pulse and decorate homogeneously the entire walls of the TiO_2 nanotubes; d) growth of nuclei to coalescence in further current pulses.

This approach seems universally applicable to the filling of TiO_2 nanotubes with metals. We filled nanotube layers with Ag, Cu, Au, and Pt using the approach described above, including bottom sealing and deposition by nuclei formation/coalescence (experimental details given in the Supporting Information). Figure 3a shows ion-milled vertical sections of the middle of the tubes, illustrating a very homogeneous filling of the tubes in each case.

After electrodeposition, I–V curves demonstrate a behavior that is consistent with the different work functions of the metals (Figure 3c) when forming a junction with TiO_2. Figure 3b shows the I–V curves for the different metals deposited into TiO_2 nanotubes. With Ag, an almost "ideal" resistor is formed, with current densities considerably higher than those of other contacts (Cu, Au, and Pt). With an increase in the work functions,[22] the heterojunctions become increasingly more diodic, in line with an increasing Schottky barrier. However, in each case, short-circuit-free junctions are formed, allowing the large-scale formation of functional interdigitated electrode arrays.

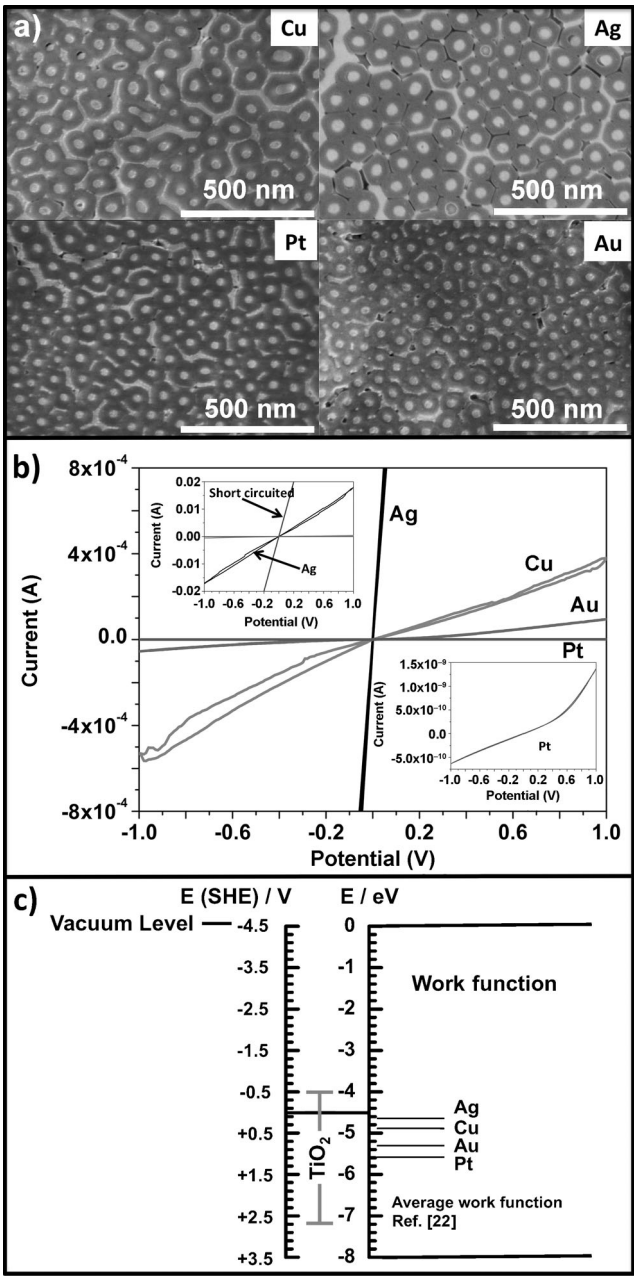

Figure 3. a) Top view SEM images of TiO_2 nanotubes filled with different metals; b) I–V curves for TiO_2 nanotubes filled with different metals; c) work functions of different metals relative to the band-edge of TiO_2.

In order to demonstrate the use of such a structure, we investigated the feasibility to obtain a memristive response from these structures, that is, to switch the bottoms of the tubes in a deposited metal/oxide/titanium substrate configuration. As the memristive effect relies on a sufficient number of oxide vacancies and their mobility,[14] the oxide needs to be adequately reduced (vacancy-rich).

To introduce oxide vacancies, we annealed the (final) device in a reducing atmosphere (10% H_2 in Ar) for various periods of time and temperatures, and measured I–V characteristics. For samples that were annealed at 400°C and more than 12 h, we observed the typical memristive (hard-switching) "butterfly" shape in the I–V curves (Figure 4). Thus, two conductivity states are established

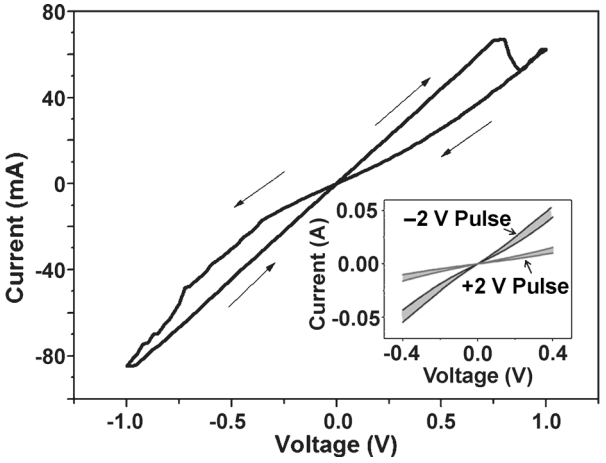

Figure 4. Memristive I–V curve obtained for the $Cu/TiO_2/Ti$ device after annealing in H_2/Ar at 400°C. Inset: I–V curves below switching threshold for high-conductivity state (established after −2 V pulse) and low-conductivity state (established after +2 V pulse). Gray fields represent the deviation obtained in 20 repeated switching cycles.

when a certain threshold voltage is passed. In our case, once a potential of approximately +0.8 V was reached, the high-conductivity state switched to a low-conductivity state. When the potential is then swept in the negative direction, reverse switching occurs at around −0.8 V. This switching effect is well maintained in repeated cycles. The inset in Figure 4 shows repeated switching using ±2 V steps and the resulting I–V curves that were measured in a nonswitching region (± 0.4 V). The results clearly demonstrate the possibility to obtain a memristive response in the sealed bottoms of anatase TiO_2 nanotube layers through an adequate reductive heat treatment. Such layers of filled nanotubes without short circuits may thus lay the ground for a novel approach to high-density storage devices with an electrode density depending on the TiO_2 nanotube diameter. The present work clearly illustrates the high potential of large-scale defect-free (sealed) nanotube layers.

In summary, we have demonstrated that uniform filling of TiO_2 nanotube layers with metals can be achieved, forming reliable large-scale interdigitated electrodes. A key requirement for short-circuit-free junctions is the sealing of stress-induced cracks in the layers of TiO_2 nanotubes. Moreover, the use of a deposition approach that is based on initially decorating the tube walls with a maximum of nuclei, followed by coalescence, is extremely successful to reach nearly 100% filling of n-type semiconductive TiO_2 nanotubes. It can be expected that these strategies are successful for virtually any n-type nanotubular material and cathodic deposition. The principle demonstrated herein is a prerequisite to construct any form of interdigitated electrode, not limited to memristors, but also in view of other solid-state devices.

Received: July 20, 2013
Published online: October 2, 2013

Keywords: electrodeposition · electrodes · sealing layer · semiconductors · TiO_2 nanotubes

[1] K. Uosaki, K. Okazaki, H. Kita, H. Takahashi, *Anal. Chem.* **1990**, *62*, 652–656.
[2] C. R. Martin, *Science* **1994**, *266*, 1961–1966.
[3] H. Masuda, K. Fukuda, *Science* **1995**, *268*, 1466–1468.
[4] D. AlMawlawi, N. Coombs, M. Moskovits, *J. Appl. Phys.* **1991**, *70*, 4421–4425.
[5] K. Nielsch, F. Muller, A. Li, U. Gösele, *Adv. Mater.* **2000**, *12*, 582–586.
[6] M. Steinhart, J. H. Wendroff, A. Greiner, R. B. Wehrspohn, K. Nielsch, J. Schilling, J. Choi, U. Gösele, *Science* **2002**, *296*, 1997.
[7] M. Jeske, J. W. Schltze, M. Thonissen, H. Munder, *Thin Solid Films* **1995**, *255*, 63–66.
[8] a) V. Zwilling, E. Darque-Ceretti, A. Boutry-Forveille, D. David, M. Y. Perrin, M. Aucouturier, *Surf. Interface Anal.* **1999**, *27*, 629–637; b) V. Zwilling, E. Darque-Ceretti, A. Boutry-Forveille, *Electrochim. Acta* **1999**, *45*, 921–929.
[9] P. Roy, S. Berger, P. Schmuki, *Angew. Chem.* **2011**, *123*, 2956–2995; *Angew. Chem. Int. Ed.* **2011**, *50*, 2904–2939.
[10] I. Paramasivam, H. Jha, N. Liu, P. Schmuki, *Small* **2012**, *8*, 3073–3103.
[11] K. Zhu, N. R. Neale, A. Miedaner, A. J. Frank, *Nano Lett.* **2007**, *7*, 69–74.
[12] J. R. Jennings, A. Ghicov, L. M. Peter, P. Schmuki, A. B. Walker, *J. Am. Chem. Soc.* **2008**, *130*, 13364–13372.
[13] J. M. Macak, B. G. Gong, M. Hueppe, P. Schmuki, *Adv. Mater.* **2007**, *19*, 3027–3031.
[14] J. J. Yang, M. D. Pickett, X. Li, D. A. A. Ohlberg, D. R. Stewart, R. T. Williams, *Nat. Nanotechnol.* **2008**, *3*, 429–433.
[15] P. Roy, D. Kim, I. Paramasivam, P. Schmuki, *Electrochem. Commun.* **2009**, *11*, 1001–1004.
[16] N. K. Shrestha, M. Yang, Y. C. Nah, I. Paramasivam, P. Schmuki, *Electrochem. Commun.* **2010**, *12*, 254–257.
[17] N. K. Shrestha, J. M. Macak, F. Schmidt-Stein, R. Hahn, C. T. Mierke, B. Fabry, P. Schmuki, *Angew. Chem.* **2009**, *121*, 987–990; *Angew. Chem. Int. Ed.* **2009**, *48*, 969–972.
[18] I. Paramasivam, J. M. Macak, P. Schmuki, *Electrochem. Commun.* **2008**, *10*, 71–75.
[19] N. Liu, H. Jha, R. Hahn, P. Schmuki, *ECS Electrochem. Lett.* **2012**, *1*, H1–H3.
[20] D. Wang, B. Yu, C. Wang, F. Zhou, W. Liu, *Adv. Mater.* **2009**, *21*, 1964–1967.
[21] H. Tang, K. Prasad, R. Sanjinbs, P. E. Schmid, F. Levy, *J. Appl. Phys.* **1994**, *75*, 2042–2047.
[22] E. H. Rhoderick, *IEE Proc.* **1982**, *129*, 1–14.

